PERGAMON

Vision Research 41 (2001) 1359–1378

Vision Research

www.elsevier.com/locate/visres

Mapping visual cortex in monkeys and humans using surface-based atlases

David C. Van Essen [a,*], James W. Lewis [a], Heather A. Drury [a], Nouchine Hadjikhani [b], Roger B.H. Tootell [b], Muge Bakircioglu [c], Michael I. Miller [c]

[a] *Anatomy & Neurobiology, Washington University, School of Medicine, 660 S. Euclid Avenue, St. Louis, MO 63110, USA*
[b] *Nuclear Magnetic Resonance Center, Massachusetts General Hospital, 149 13th Street, Charlestown, MA 02129, USA*
[c] *Center for Imaging Science, Whiting School of Engineering, The Johns Hopkins University, 221 Barton Hall, 3400 N. Charles Street, Baltimore, MD 21218-2686, USA*

Received 21 September 2000; received in revised form 30 January 2001

Abstract

We have used surface-based atlases of the cerebral cortex to analyze the functional organization of visual cortex in humans and macaque monkeys. The macaque atlas contains multiple partitioning schemes for visual cortex, including a probabilistic atlas of visual areas derived from a recent architectonic study, plus summary schemes that reflect a combination of physiological and anatomical evidence. The human atlas includes a probabilistic map of eight topographically organized visual areas recently mapped using functional MRI. To facilitate comparisons between species, we used surface-based warping to bring functional and geographic landmarks on the macaque map into register with corresponding landmarks on the human map. The results suggest that extrastriate visual cortex outside the known topographically organized areas is dramatically expanded in human compared to macaque cortex, particularly in the parietal lobe.

Keywords: Architectonic; Maps; Probabilistic; Visual areas; Visual topography

1. Introduction

Higher visual processing in primates involves a large expanse of visual cortex that occupies much of the occipital, parietal, temporal, and even frontal lobes. It is of fundamental neurobiological importance to know how the visual cortex is subdivided into anatomically and functionally distinct areas, just as knowledge about the earth's geographical and political subdivisions is critical to fields such as political science and history. Numerous studies over the past century have revealed that visual cortex contains a complex mosaic of distinct areas that differ from one another in a variety of characteristics, including architecture, connectivity, topographic organization, and/or functional properties (Felleman & Van Essen, 1991; Rockland, Kaas, & Peters, 1997; DeYoe, 2001). On the one hand, this represents vital progress on basic issues of cortical cartography. On the other hand, the objective of accurately and completely charting all of visual cortex remains far from complete, even for the macaque monkey and other intensively studied non-human primates. For human visual cortex, which is naturally of special interest, our understanding remains much more fragmentary, even though new neuroimaging methods have led to rapid recent progress. Altogether, our overall knowledge about visual-cortical organization arguably corresponds to that which cartographers of the earth's surface had attained around the end of the 16th century.

Of the many challenges involved in deciphering visual-cortical organization, three are particularly relevant to the present study. First, the distinctions between neighboring visual areas are often subtle, even when using the most sensitive techniques available. Identifying clear boundaries between areas is especially problematic for the mosaic of relatively small visual areas that lie beyond V1 and V2, which are the largest

* Corresponding author. Tel.: +1-314-3627043; fax: +1-314-7473436.
E-mail address: vanessen@v1.wustl.edu (D.C. Van Essen).

0042-6989/01/$ - see front matter
PII: S0042-6989(01)00045-1

areas and the easiest to delineate. Consequently, a variety of different partitioning schemes remain in widespread use for describing cortical subdivisions in extrastriate visual cortex. Second, in many species, including humans and macaques, most of the visual cortex lies buried within complex and irregular sulci. The depth and irregularity of cortical convolutions has been a chronic impediment to visualizing spatial relationships among the complex mosaic of visual areas. Third, there is a marked variability in the pattern of folding from one individual to the next (geographic variability) and in the size and shape of visual areas and their location relative to geographic landmarks (functional variability). Taken together, geographic and functional variability exacerbate the visualization problems arising from the irregularity of cortical convolutions and make it harder to assess the consistency of subtle areal boundaries.

In this report, we focus on *surface-based atlases* as a powerful and flexible approach for analyzing cortical organization in the face of the technical challenges noted in the preceding paragraph. Recent advances in computerized brain mapping make it feasible to generate surface-based atlases that have many advantages over conventional stereotaxic atlases, which heretofore have been the most common substrate for bringing data from individual experiments into a common framework (e.g. Talairach & Tournoux, 1988). The advantages of surface-based atlases fall into six general areas, each of which is illustrated in this report.

1. *Visualization*. A surface reconstruction can be viewed in a variety of complementary configurations, ranging from its original 3-D (fiducial) configuration to flat maps that allow the entire cortical surface to be seen in a single view. Each configuration has certain advantages for visualization or analysis, and there is no need to adopt any particular one as an exclusive standard because available software allows rapid interchanging between different configurations. It is now feasible to reconstruct and flatten surfaces routinely and accurately from cryosection or structural MRI data (Drury et al., 1996a; Dale, Fischl, & Sereno, 1999; Fischl, Sereno, & Dale, 1999a; Van Essen et al., 1999; Goebel, 2000; Kiebel, Goebel, & Friston, 2000; Wandell, Chial, & Backus, 2000).
2. *Surface-based coordinates*. Locations within the cerebral cortex can be precisely and concisely described using surface-based coordinates, which are inherently advantageous over conventional stereotaxic coordinates because they respect the topology of the cortical sheet (Drury et al., 1996a; Sereno, Dale, Liu, & Tootell, 1996). Spherical coordinates of latitude and longitude are particularly attractive in this regard for cerebral cortex, just as they are for maps of the earth's surface (Fischl, Sereno, Tootell, & Dale, 1999b; Drury, Van Essen, Corbetta, & Snyder, 1999a; Drury, Van Essen, & Lewis, 1999b).
3. *Surface-based warping*. A critical issue in dealing with individual variability is to bring data from many individuals as accurately as possible into register with an atlas. Surface-based warping is a natural strategy for attacking the registration problem because it allows individual hemispheres to be deformed to an atlas map while preserving neighborhood relationships on the cortical sheet (Van Essen, Drury, Joshi, & Miller, 1998; Drury et al., 1999a,b; Fischl et al., 1999b).
4. *Layering of maps*. A computerized atlas can incorporate unlimited amounts of information of many different types, all in a common spatial coordinate system. Analysis of these data can be greatly aided by treating each data set (e.g. visual areas in a particular partitioning scheme) as a separate layer that can be visualized on its own or in combination with selected other layers. This can greatly facilitate the evaluation of commonalities as well as differences between partitioning schemes or other types of experimental data.
5. *Probabilistic maps*. It would be ideal if maps of different hemispheres could be brought into an exact register on an atlas. Unfortunately, perfect registration is neither a realistic objective nor even a well-defined concept, in view of the combined individual variability in geographic and functional organization characteristic of cerebral cortex. Instead, the objectives of the registration process should be to maximize the quality of registration and to represent the residual uncertainty and variability for data mapped to an atlas. These objectives can be effectively addressed by surface-based warping of many individual hemispheres to an atlas and by combining the resultant data sets into probabilistic atlases for depicting the likelihood that any given cortical area will be encountered at each location on an atlas map.
6. *Interspecies comparisons*. Comparisons between humans and various non-human primates are of considerable interest because there are numerous commonalities in functional organization, particularly for the topographically organized visual cortex in the occipital lobe. However, detailed analyses are impeded by major interspecies differences in the relative sizes of different areas and in their location relative to major geographic landmarks. Surface-based warping provides a natural strategy for addressing these impediments and for evaluating the degree to which there is a common organizational plan in terms of the identities of visual areas and their topological relationships with one another across the cortical sheet.

2. Methods

2.1. Surface reconstructions and identification of visual areas

Surface-based analyses were carried out on experimental data acquired in several previously published studies. The surface-based atlas for the macaque, adapted from Carman, Drury, and Van Essen (1995) and Drury et al. (1996a) was based on manually drawn contours through layer 4 on photographs of Nissl-stained histological sections through a normal macaque right hemisphere (species and body weight not known). This choice for an atlas is in some respects arbitrary, but as other surface-based atlases become available, it will be relatively straightforward to transform data sets from one atlas to another. The estimated locations of areal boundaries from the Felleman and Van Essen (1991) partitioning scheme were initially delineated on an enlarged physical model of the same hemisphere and then transposed onto the digital surface-based atlas. For the human atlas, we used the Visible Man surface-based atlas (Van Essen & Drury, 1997), generated from contours traced through the mid-cortical thickness on images of a cryosectioned brain (Spitzer, Ackerman, Scherzinger, & Whitlock, 1996). This brain was transformed to Talairach stereotaxic space using Spatial Normalization software (Lancaster et al., 1995). The pattern of convolutions in this hemisphere is within the normal range reported by Ono, Kubick, and Abernathey (1990) and Steinmetz, Furst, and Freund (1990).

2.2. Surface-based analysis and visualization

A probabilistic map of macaque visual cortex was generated using architectonic data from the anatomical study of Lewis and Van Essen (2000a). Surface reconstructions of individual hemispheres were generated by tracing layer 4 contours on histological sections and were reconstructed and flattened as described in Drury et al. (1996a). Core regions of architectonic subdivisions were identified on histological sections (based on myeloarchitecture, SMI-32 immunoreactivity, and cytoarchitecture) and entered along with the layer 4 contours used for the computerized surface reconstructions. Boundary contours enclosing each architectonic subdivision were drawn using Caret (Computerized Anatomical Reconstruction and Editing Toolkit) surface visualization software (Drury et al., 1996a, 1999a). The surface was then ''painted'' by a method that automatically assigns an appropriate areal identity to nodes of the surface reconstruction that were surrounded by each closed boundary and stores these assignments in a ''paint'' file associated with that surface. A similar process was used to identify geographic regions (gyral boundaries, sulcal fundi and cortical lobes) and to paint regions of buried cortex.

A probabilistic map of human visual cortex was generated using data taken from a recent fMRI study of topographically organized visual areas (Hadjikhani, Liu, Dale, Cavanagh, & Tootell, 1998). Methods for surface reconstruction, cortical inflation and flattening, and mapping of fMRI data are as described by Dale et al. (1999) and Hadjikhani et al. (1998). Images of flat maps with areal boundaries and relevant geographic boundaries were imported into Caret, where boundary tracing and subsequently processing steps were carried out.

2.3. Surface-based warping

Flat maps of individual hemispheres containing experimental data (''source maps'') were deformed to the surface-based atlas (''target map'') using a fluid-based deformation method (Joshi, 1997; Van Essen, Drury, Joshi, & Miller, 1998). Deformations were constrained by explicitly defined contours presumed to represent corresponding locations on the source and target maps. Registration contours were based on geographic landmarks for the macaque map deformations and on a combination of geographic and functional landmarks for the human map deformations. The deformation method brings corresponding points along each registration contour into alignment while preserving surface topology (i.e. avoiding folding of the deformed surface onto itself) and minimizing the aggregate distortions (shear and dilation) in regions between landmarks (Joshi, 1997). Additional contours carried passively along during the deformation included a variety of geographic and functional landmarks, plus a gridwork used to assess the nature and extent of local deformations required to achieve registration.

Deformations of spherical maps were carried out using a modification of this algorithm that applies to data sets on the sphere (Bakaciroglou, Joshi, & Miller, 1999). The mapping from macaque to human cortex involved very large deformations constrained by primary landmarks that are inherently sparse (i.e. separated by large distances across the cortical surface). To achieve a satisfactory deformation without undue shear or buckling, it was necessary to supplement the primary landmarks by an array of secondary landmarks placed in the intervening regions by a method of triangular interpolation. Corresponding triplets of primary landmarks were identified on both the source and target maps, and the geometric centers of these triangles were projected onto the spherical map to define a set of secondary landmarks. Additional landmarks were generated using secondary as well as primary landmarks to define corresponding triplets on each map. The source map was deformed to the target map by interpolating through a set of intermediate steps, to avoid large deformations in any single step. The targets for the

intermediate stages were determined by interpolating linearly between corresponding pairs of source and target landmarks. The output of each intermediate deformation (including passively deformed contours as well as landmark points) was used as the input for the next stage of deformation.

2.4. Probabilistic atlases

For each map deformed to the atlas, the deformed boundaries of identified visual areas were used to paint the atlas surface, by the areal assignment process described above. This process was carried out on multiple hemispheres, thereby generating a composite atlas file in which each node contained areal assignments for each of the hemispheres contributing to the probabilistic atlas. A visualization option in Caret assigned colors to each node that depended on both the area identity and the fraction of cases in the atlas sharing that identity.

3. Results

3.1. Analyses of macaque visual cortex

3.1.1. Surface-based atlas for the macaque

Fig. 1 shows a surface-based atlas for the macaque monkey that is a compendium of many types of information and can be viewed in a variety of display formats. The upper panels show representations of cortical geography on three different configurations: the three-dimensional "fiducial" surface running midway through the cortical thickness (Fig. 1A); a spherical surface (Fig. 1B); and a flat map in which cuts were made to reduce distortions in surface area (Fig. 1C). Buried cortex is displayed in darker shades and cortical lobes in different pastel colors. In addition, surface-based coordinates of latitude and longitude were generated on the spherical map and projected to the other two configurations, much as is done for maps of the earth's surface. The bottom panels show maps of functional organization, based on the cortical partitioning scheme of Felleman and Van Essen (1991). These are displayed on the fiducial surface (Fig. 1D), a flat map of the entire hemisphere (Fig. 1E) plus an expanded flat map that includes labels for the visual areas of the occipital, parietal, and temporal lobes (Fig. 1F). This partitioning scheme represents a synthesis from many previous anatomical and physiological studies; boundaries in the atlas are only approximations to the actual boundary locations in the experimental hemispheres where the data were originally acquired.

Besides the spherical coordinates displayed on the geographic maps, Fig. 1 also shows a complementary surface-based coordinate system based on Cartesian coordinates on the flat map. The ventral tip of the central sulcus serves as a convenient, consistently recognizable landmark used as the origin for the Cartesian coordinates and as the lateral pole for the sphere. Any given location on the atlas can be concisely and precisely specified by its spherical coordinates of latitude and longitude (ϕ, θ) or by its Cartesian coordinates. For example, Fig. 1 contains two reference markers at sites useful for comparisons made with subsequent figures. Reference marker "a", placed in area VIP along the fundus of the intraparietal sulcus, can be pinpointed by its Cartesian coordinates of [− 20, + 10] map-mm and its spherical coordinates of [+ 35°, 150°]. Reference marker "b", placed in area CITv on the inferior temporal gyrus, has Cartesian coordinates of [− 20, − 30] map-mm and spherical coordinates of [− 12°, 275°].

3.1.2. Probabilistic atlas of macaque architectonic areas and zones

There are numerous alternative partitioning schemes for macaque visual cortex besides the particular scheme shown in Fig. 1. Comparisons between schemes can be carried out most accurately when surface reconstructions are available for the hemispheres in which the experimental data were acquired. For example, Fig. 2 illustrates two cases from a recent anatomical study in which architectonic subdivisions were charted over much of the hemisphere, based on a combined analysis of myeloarchitecture, cytoarchitecture, and immunoreactivity for SMI-32 (Lewis & Van Essen, 2000a). Fig. 2A–D shows results from one hemisphere (Case 1) displayed on a surface reconstruction covering most of the hemisphere (all but the frontal pole anteriorly and area V1 posteriorly). Architectonic subdivisions are displayed on a fiducial 3-D surface (Fig. 2A), an inflated

Fig. 1. Surface-based atlas of macaque visual cortex based on a reconstruction of cortical layer 4 (see Section 2). Panels (A)–(C) show maps of cortical geography (lobes in pastel shades, buried cortex in darker shades). (A) Lateral view of the fiducial surface, with spherical coordinates and lateral pole at tip of central sulcus. (B) Lateral view of the cortex mapped to a sphere including lines of constant latitude and longitude. (C) Flat map with spherical coordinates on each surface, and Cartesian coordinates are shown in the background. Panels (D)–(F) show maps of the Felleman & Van Essen (1991) partitioning scheme D. Lateral view of the fiducial surface, with areas associated with visual processing indicated in different colors; non-visual areas outlined along boundaries. (E) Flat map of entire right hemisphere. (F) Expanded flat map of posterior cortex, with all 32 visual areas labeled. Marker points (a = [− 20, + 10] map-mm; b = [− 20, − 30] map-mm) illustrate the corresponding locations on each panel. These data can be downloaded for viewing in Caret by making a hyperlink connection to http://stp.wustl.edu/sums/sums.cgi?specfile = 2001.03-02.790.R.MACAQUE_ATLAS.spec

map (Fig. 2B), a flat map of the entire reconstruction (Fig. 2C), and an expanded flat map of visually related subdivisions (Fig. 2D). Fig. 2E shows an expanded map of parietal and dorsal occipital cortex from a different

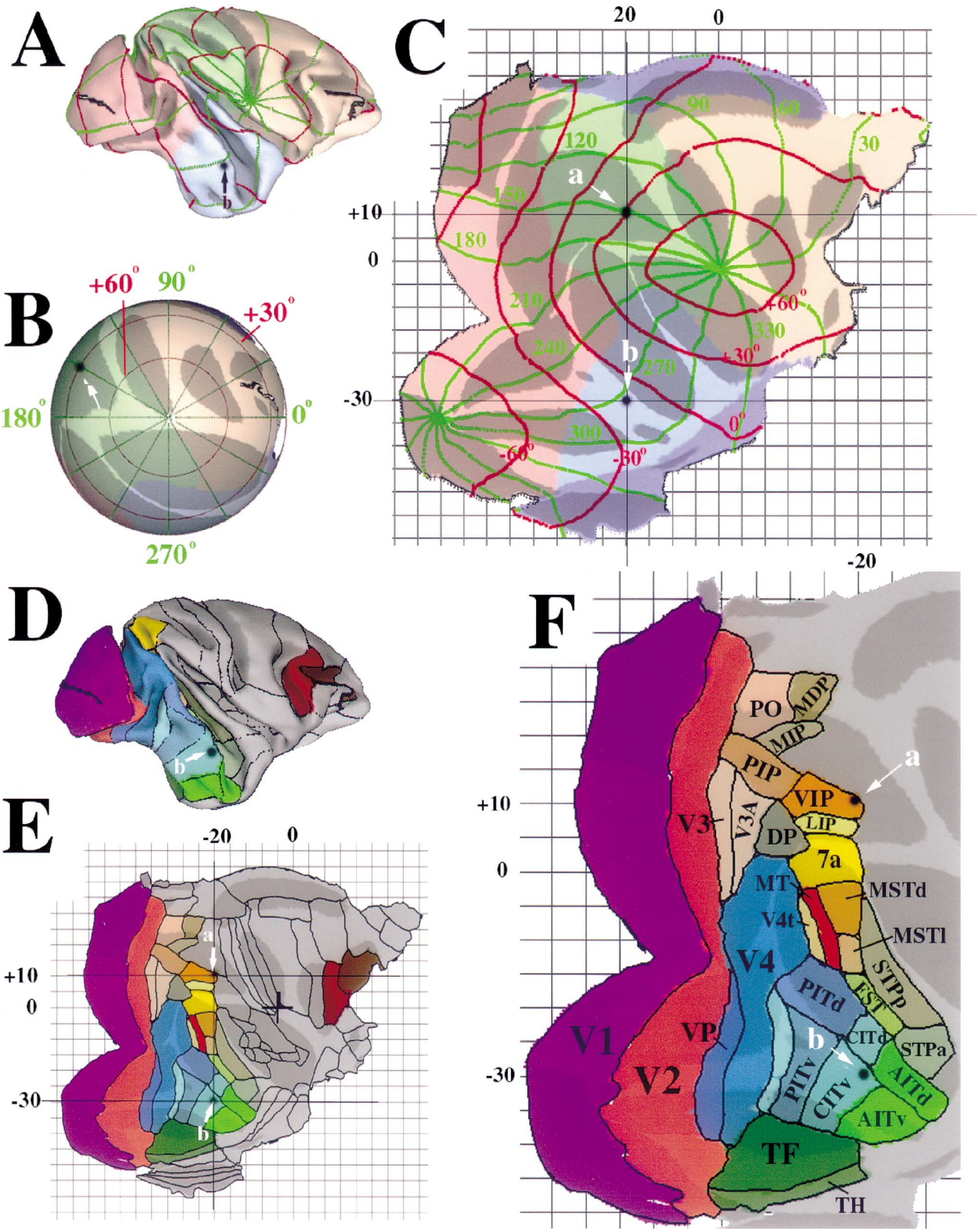

Fig. 1.

hemisphere (Case 2). On all panels, solid lines outline the architectonically consistent core region of each subdivision. The gaps between core regions represent transition regions, which are narrow in many regions (<1 mm) but extend over several millimeters in regions where the architectonic distinctions between subdivisions are subtle or were obscured by the sectioning plane (coronal) used in this analysis. Regions implicated in visual processing are shaded using a coloring scheme similar to that in Fig. 1.

The architectonic subdivisions shown in Fig. 2 were consistently recognizable across many hemispheres, so they presumably represent neurobiologically significant aspects of cortical organization. However, the consistency of architectonic transitions per se does not imply that each subdivision is a truly distinct cortical area: well-defined cortical areas can be internally heterogeneous, as is well known for the cytochrome oxidase blobs of V1 and stripes of V2 (Horton & Hubel, 1991; Tootell & Hamilton, 1989; DeYoe, Hockfield, Garren, & Van Essen, 1990). Accordingly, we classified each architectonic subdivision in Fig. 2 as either an *area* or a *zone*, based on the aggregate evidence available from existing anatomical and physiological studies. For example, we regard LIPd (yellow) and LIPv (red) as distinct visual *areas*, based on differences in physiology and connectivity as well as architectonics, even though, in the scheme of Fig. 1, this approximate region had been designated as a single larger area, LIP. In contrast, for other subdivisions identified as *zones*, there is insufficient evidence at present to resolve whether they represent separate areas or internal architectonic heterogeneity. In our view, this uncertainty applies to zones VIPl and VIPm within area VIP (both colored dark orange); zones MSTdp, MSTm, MSTdl within area MST (all light orange); zones V4ta and V4tb within area V4t (yellow–orange); and zone LOP in between areas LIPv and V3A. Altogether, the maps in Fig. 1 contain 23 architectonically identified visual areas and a total of 31 subdivisions (zones and areas combined).

Surface-based coordinates can aid in comparing different partitioning schemes (e.g. Fig. 1 vs. Fig. 2) and assessing individual variability within a given partitioning scheme (e.g. Fig. 2D vs. Fig. 2E). One approach is to ascertain whether locations having identical map coordinates represent similar geographic and/or functional regions in different hemispheres. For example, the Cartesian map location of $[-20, +10]$, at the tip of area VIP in the intraparietal sulcus on the atlas map (Fig. 1C and F), lies at a similar location in Case 1 (point a′, near the tip of zone VIPl) and in Case 2 (point a″, on the anterior half of zone VIPm).

In contrast, the Cartesian map location of $[-20, -30]$, in area CITv on the inferior temporal gyrus of the atlas map, lies in architectonic area TEa/m, within the superior temporal sulcus, of Case 1 (point b′) and also Case 2 (data not shown). In regions, where there are differences in both the partitioning schemes and the geographic location associated with particular map coordinates, it is difficult to analyze and interpret these differences using only side-by-side comparisons of maps.

To facilitate systematic comparisons among complex data sets represented on different maps, it is desirable to bring all of the data into register with a surface-based atlas. Our approach to this involves surface-based warping, using the landmark-based fluid deformation method illustrated in Fig. 3. The objective is to deform the "source" map for one case (Case 1 in Fig. 3A) to bring it into registration with the "target" map (the atlas map in Fig. 3D). The registration contours used to constrain the deformation include geographic landmarks along the fundi of major sulci, plus the perimeter of the source map and corresponding contours on the target map. Fig. 3B shows the shape of the source map after deformation to the target, along with a deformed gridwork that reveals the pattern of shear and dilation of the initially Cartesian gridwork in Fig. 3A. Even in maximally deformed regions, there is no tangling of the gridwork, signifying that the deformation has not compromised the topology of the cortical map. The deformation field is illustrated in a different format in Fig. 3C, using vectors to represent the magnitude and direction in which regularly spaced grid points (at intervals of 10 map-mm) were translated by the deformation. For example, the marker point in the intraparietal sulcus (a′) was translated 4 map-mm up and to the left, whereas the marker point in the superior temporal sulcus (b′) was translated 5 map-mm up and to the right. Fig. 3E shows the deformed registration contours (thick lines) and sulcal boundaries (thin lines) overlaid on a map of cortical geography on the target atlas. There is close registration between the contours on the atlas map (Fig. 3D) and those on the deformed source map (Fig. 3E), implying that the algorithm successfully matched the landmarks used to constrain the deformation. More importantly, the deformation markedly improved the registration of regions lying between these landmarks. This is demonstrated by the alignment between sulcal boundaries of the deformed source map (thin lines in Fig. 3E) and the corresponding sulcal boundaries on the target map (boundaries of the shaded regions in Fig. 3D). The agreement is good for most major sulci, including the central sulcus (CeS) and superior temporal sulcus (STS). Also, the deformation preserves the positioning along the length of each sulcus. For example, deformed point a′ is located posteriorly in the atlas intraparietal sulcus (IPS) just as it is in the Case 1 map, in contrast to the more anterior position of the same map coordinates (marker point a) in the atlas. In a few

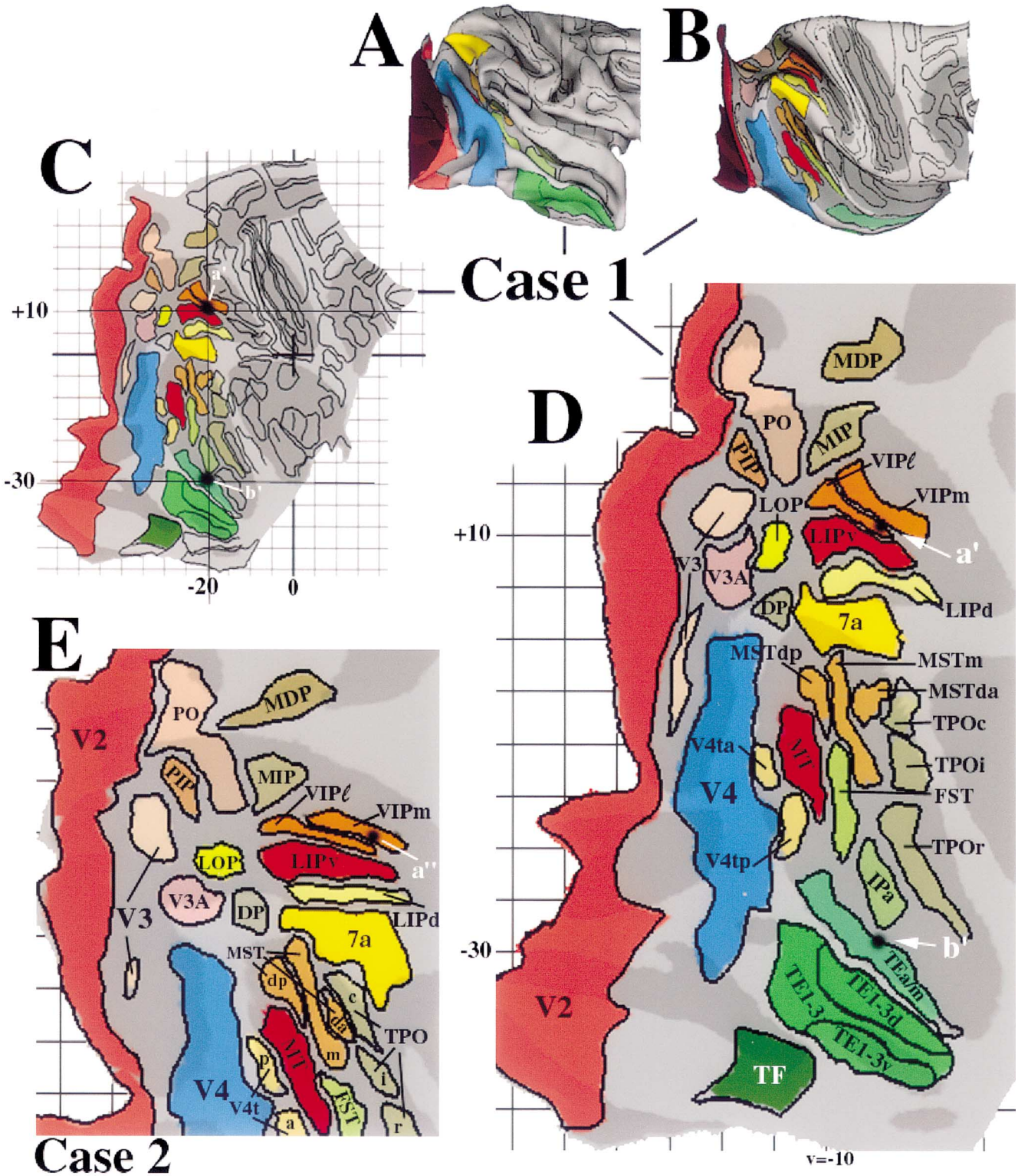

Fig. 2. Maps of visual areas and zones in occipital, temporal, and parietal cortex in two cases from the architectonic study of Lewis and Van Essen (2000a). Panels (A)–(D) show architectonic subdivisions from Case 1 (95DR). (A) Lateral view of fiducial surface reconstruction, including all of the right hemisphere except the frontal pole and area V1. (B) Dorso-lateral view of inflated surface. (C) Flat map of the entire reconstruction. (D) Flat map of posterior cortex with visual areas labeled. Area 7a was identified as the posterior half of area 7, as charted by Lewis and Van Essen, as their study did not distinguish between visually related area 7a and somatosensory-related 7b owing to local tissue damage associated with anatomical tracer injections. (E) Flat map of dorsal posterior cortex from Case 2 (94CR) of Lewis and Van Essen (2000a). The arrangement of architectonic subdivisions is broadly similar to that in Case 1, but there are numerous minor differences in the size, shape, and location of individual areas and zones. To download these data, connect to http://stp.wustl.edu/sums/sums.cgi?specfile = 2001-02-28.95D.R.Architectonic.spec

regions, such as the inferior occipital (IOS) and occipito-temporal (OTS) sulci, the registration of geographic boundaries is less precise, because of greater disparities in the local folding patterns. If a different set of geographic landmarks were used to constrain the deformation (e.g. the margins of sulci as well or instead of sulcal fundi), the deformation patterns would differ in various details, though not by a large amount, given the overall similarity of the folding patterns in these two cases.

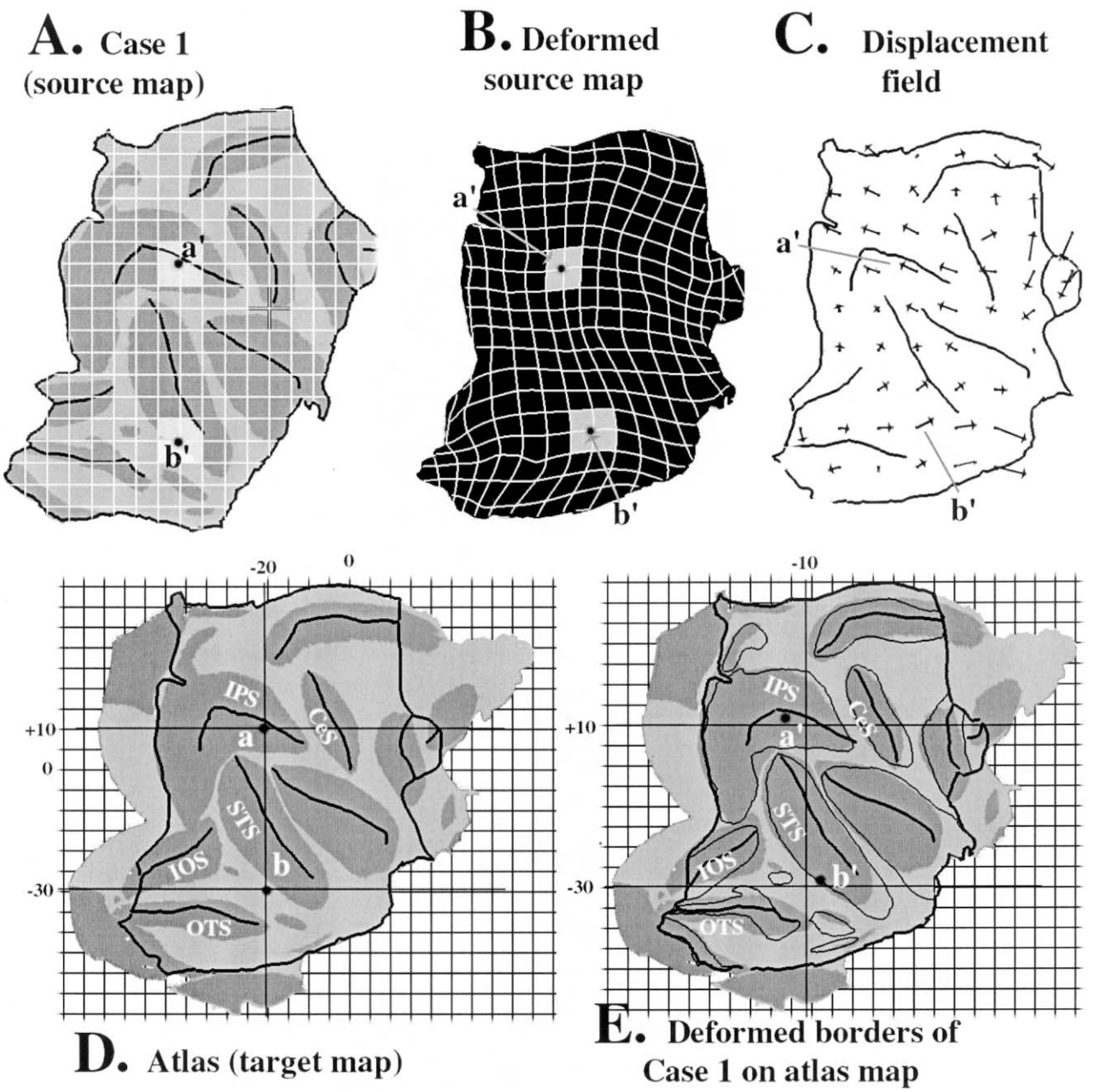

Fig. 3. Surface-based warping from an individual flat map to the macaque atlas. (A) Flat map of Case 1. Shading indicates cortical geography; black lines indicate the landmark contours used to constrain the deformation (along sulcal fundi and along the map perimeter); and white lines indicate grid lines at intervals of 5 map-mm. Gray boxes highlight the reference marks ($a' = [-20, +10]$; $b' = [-20, -30]$). (B) Pattern of grid lines after deformation of Case 1 to bring it into register with the target atlas map in (D). Gray boxes highlight the locations of deformed marker points a′ and b′. (C) Displacement field for selected grid points (at intervals of 10 map-mm). Arrow bases indicate the grid positions in the source map, and arrow tips indicate the location of grid points in the deformed source map. For example, displacements are largely to the right in the lower part of the map and largely to the left in the upper left of the map. (D) Map of geography (shading) and target registration contours (black lines) on the atlas map. Reference marks are identical to those in Fig. 1 ($a = [-20, +10]$; $b' = [-20, -30]$). (E) Contours from the deformed source map (black lines) and deformed reference marks a′, b′ are overlaid on the target atlas map.

Surface-based warping was applied to five cases in which architectonic subdivisions had been charted over most of the visual cortex (Lewis & Van Essen, 2000a). A composite representation containing all five deformed maps registered to the surface-based atlas provides a substrate for a variety of analyses and visualization options. One option is to select any of the individual maps for visualization after deformation to the atlas. For example, Fig. 4A shows a map of Case 1 after deformation to the atlas. Individual areas on the deformed map are shifted in location and modified in size and shape compared to their starting configuration in Fig. 2C and D, but only to the degree expected from the deformation field shown in Fig. 3.

Another set of viewing options involves probabilistic maps that provide a systematic representation of both the consistency and the residual variability in the position of each architectonic area after deformation to the atlas. A probabilistic map that includes all of the architectonically identified visual areas and zones from the Lewis and Van Essen study is shown as a flat map in Figure 4B,C and on a lateral view of the hemisphere in Figure 4E. Each atlas location is assigned a color representing both the areal identity at that location and the fraction of cases in the population contributing to that identity. For example, the horizontal white arrow points to a location [+10°, 200°] identified as area V4 on all five deformed maps and hence colored bright blue. The nearby vertical white arrow points to a location [+45°, 225°] that is a pale (less saturated) blue because it was associated with V4 in only one case. Appropriate hybrid colors were assigned to locations that were associated with more than one visual area in the population of maps deformed to the atlas (e.g., area V4 in some cases and adjoining area TE1-3 in others). The different gradations of saturation are difficult to distinguish in many regions. For making quantitative determinations of probabilities, it is preferable to use the freely available digital atlas (see figure legend) and the associated Caret visualization software, which includes options for direct readout of areal assignments at each node.

Fig. 4C shows boundaries that were drawn midway along the transitional regions between adjoining areas. For a few of these boundaries (areas VP, VOT, and TF), the areas were not identified architectonically by Lewis and Van Essen but instead were based on the Felleman & Van Essen scheme (Fig. 1). In Fig. 4D and F, the outlined regions are filled with solid colors, yielding a summary representation showing the most likely extent of each visual area and zone. Altogether, the map contains 35 subdivisions, of which 28 can be regarded as distinct visual areas using the criteria of Lewis and Van Essen (2000a). This summary map provides a convenient substrate for comparison with other schemes. For example, Fig. 4G shows a map of parietal-temporal cortex with an overlay between the older Felleman and Van Essen scheme (outlines, black labels) and the new, predominantly architectonic partitioning scheme (solid colors, white labels). Although the maps are broadly similar, there are a few substantial differences as well as numerous minor differences. For example, area LIP in the Felleman & Van Essen scheme corresponds with area LIPd, not to the combined LIPd and LIPv of Lewis & Van Essen. Area VIP of Felleman & Van Essen overlaps zone VIPl but not zone VIPm, and overlaps even more extensively with area LIPv of Lewis & Van Essen. Both schemes identify the area MT on the posterior bank of the STS, but it is centered several millimeters more lateral (to the left on the flat map) in the Lewis and Van Essen scheme. Though modest in magnitude, such quantitative differences can be important in a variety of contexts, particularly for areas such as MT that are targets of intensive study by visual neurophysiologists and anatomists.

3.1.3. Probabilistic surface-based atlas of human visual cortex

Over the past decade, non-invasive neuroimaging studies, particularly functional and structural MRI, have revealed numerous topographically organized visual areas in human occipital cortex. There are many striking similarities in the pattern of topographic organization compared to that of the macaque, but there are many significant differences as well.

We have used the Visible Man data set as the substrate for a surface-based atlas onto which data from many individuals can be brought into register. Fig. 5 illustrates several types of information about the extent of visual cortex and the location of individual areas. These are displayed on different configurations, including fiducial 3-D views (Fig. 5A, B), flat maps (Fig. 5C, D), and inflated surfaces (Fig. 5Y, Z). The white outlines in panel C indicates the estimated boundaries of Brodmann's cytoarchitectonic areas (Drury et al., 1999a). The dark shading in Fig. 5A–D indicates the approximate overall extent of extrastriate visual cortex, estimated from a combination of PET, fMRI, and lesion studies to include Brodmann's areas 18–21, 37, 39, and 7 (Drury et al., 1999a). By this estimate, roughly a third of human cerebral cortex is associated with visual processing. The lightly shaded region in Fig. 5A–C indicates the average extent of area V1, which occupies only about 3% of human neocortex (in contrast to its 10% occupancy in the macaque, evident in Fig. 1E). The black contours indicate the approximate range of individual variability in the V1/V2 boundary, which runs along the lips of the calcarine sulcus (CaS) in some hemispheres, but more than 2 cm away from the sulcus in others (Rademacher, Caviness, Steinmetz, & Galaburda, 1993; Amunts, Malikovic, Schormann, & Zilles, 2000). Fig. 5D–F shows the estimated location

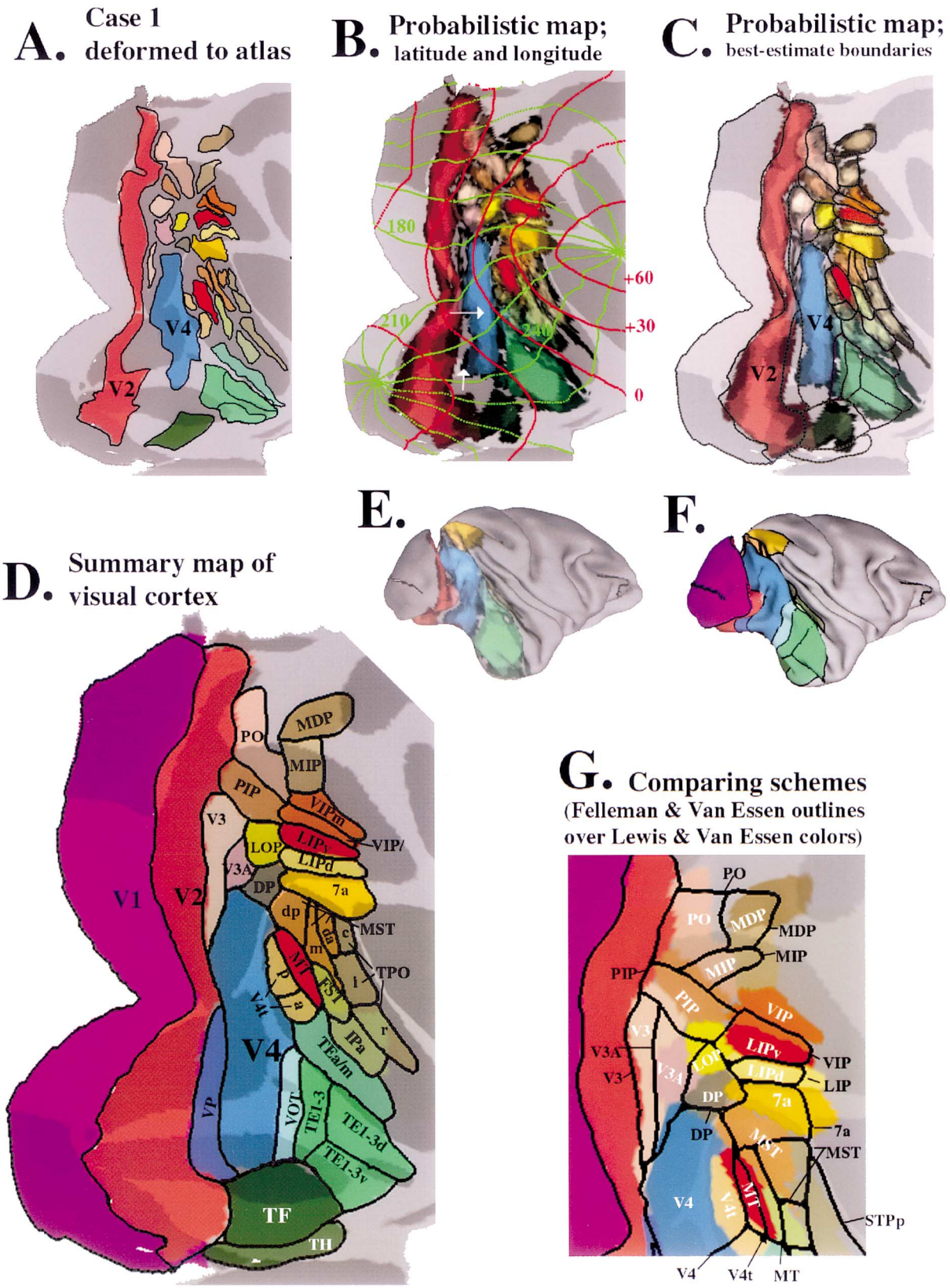

Fig. 4.

of six topographically organized visual areas (V1, V2, V3, V3A, VP, and V4v), adapted from an analysis of previous PET and fMRI studies by Van Essen and Drury (1997). Areal boundaries were estimated from

the average width of each area, as displayed on cortical flat maps (Sereno et al., 1995; DeYoe et al., 1996) and were transposed onto the Visible Man flat map using the V1/V2 boundary as a reference landmark.

To generate a probabilistic atlas of human visual areas, we used data from the fMRI visuotopic mapping study of Hadjikhani et al. (1998). Fig. 6A shows a flat map of one exemplar hemisphere from that study, showing the boundaries of eight visual areas, including the six shown in the preceding figure (V1, V2, V3, V3A, VP, and V4v), plus area V8 and MT+ (the motion-responsive region that includes area MT and part of the adjoining MST complex). In dorsal extrastriate cortex, area V3A contains a complete representation of the contralateral hemifield, in contrast to the lower-field only representation in neighboring area V3. The lower-field (−) representation of V3A adjoins that of V3; its upper-field (+) representation is to the right on the flat map. In ventral extrastriate cortex, area V8 contains a complete hemifield representation, in contrast to the upper-field only representations in neighboring areas V4v and VP. Both the lower-field and upper-field representations of V8 adjoin V4v, with the lower-field representation (−) more posterior (up on the map), the upper-field representation (+) more anterior (down on the map), and the foveal representation (*) located away from V4v (to the right on the map).

In order to bring this map into register with the atlas using landmark-based surface-based warping, it is first necessary to identify appropriate landmarks on the source and target maps. To constrain the deformation, we elected to use the boundary of area V1 as a functionally defined landmark, along with several geographically based landmarks (see figure legend) rather than using exclusively geographic landmarks as was done for the macaque probabilistic atlas. Fig. 6B shows the visual areas from the exemplar case after deformation to the atlas, using a coloring scheme similar to that used for the macaque.

Visuotopic maps from four hemispheres analyzed by Hadjikhani et al. (1998) were combined to form a probabilistic map using the same approach described above for the macaque. The results are shown on flat maps (Fig. 6C–E), an inflated map (Fig. 6F), a sphere (Fig. 6G), and fiducial 3-D surfaces from lateral (Fig. 6H) and ventral (Fig. 6I) views. To reduce overlap, the probabilistic maps for one set of areas (group 1, including V1, V3, VP, and V8) are shown in Fig. 6C, are shown in Fig. 6B, with a map of the complementary set of areas (group 2, including V2, V3A, V4v, and MT) is shown in Fig. 6D. (As in Fig. 4, the saturation differences in this figure are difficult to read quantitatively, but this information can be readily accessed using freely available visualization software.) Fig. 6E shows prototypic boundaries drawn along the transitional region between neighboring areas. By this reckoning, area V4v maps mainly to the collateral sulcus of the atlas, centered at spherical coordinates of [−45°, 230°]. Since the Visible Man atlas has been transformed to Talairach stereotaxic space, this location can also be expressed by its Talairach coordinates of [26, −75, −3]. Area V8 maps mainly to the fusiform gyrus and is centered at spherical coordinates of [−40°, 235°] and Talairach coordinates of [24, −68, −8]. For comparison, the Talairach coordinates for the color-selective ventral extrastriate region are [+26, −67, −9], as estimated by Hadjikhani et al. (1998) by averaging across several studies. This is much closer to the center of V8 than V4.

3.1.4. Interspecies comparisons

Similarities in the arrangement of visuotopic areas and in the types of functional specializations in human and macaque occipital cortex make it likely that there are genuine homologies (i.e. common evolutionary lineages) for a number of visual areas, including V1, V2, MT, and probably also V3, VP, and V3A. However, in regions progressively farther away from area V1 (the most compelling homologue), it is increasingly difficult to assess other candidate homologies. The difficulties arise from several factors, including (i) the large differences in the pattern of convolutions; (ii) differences in the location of V1 and other presumed homologues relative to the calcarine sulcus and other geographic landmarks identifiable in both species; (iii) differential expansion of extrastriate cortical areas, as evidenced by the fact that cerebral cortex is about 10-fold greater in surface area in humans compared to macaques, yet human area V1 is only twice that of the macaque (see

Fig. 4. Probabilistically based maps of macaque visual cortex. (A) Map of visual areas from Case 1 after deformation to the atlas. Shading represents cortical geography (sulci) of the atlas, not the deformed source map. The coloring of visual areas is identical to that in (D) where areas are labeled (and also to that in Fig. 2). (B) Probabilistic map of visually related architectonic subdivisions derived from 5 hemispheres studied by Lewis and Van Essen (2000a) along with latitude and longitude iso contours. The same probabalistic map of visual areas and zones shown in the preceding panel, along with contours indicating the estimated boundaries of each area and zone based on the overlap between adjacent subdivisions on the probabilistic map. (D) summary map of visual cortical areas and zones based mainly on the Lewis and Van Essen partitioning scheme but also including several visual areas from the Felleman and Van Essen (1991) scheme (VP, VOT, and TH). (A) Probabilistic map for all areas shown on a lateral view of the hemisphere. (F) Summary map of all visual areas shown on a lateral hemispheric view. (G) Overlay map showing the Lewis and Van Essen summary map [same as (D)] in colors with areas identified in white and the Felleman and Van Essen scheme (same as Fig. 1) as outlines, with areas identified in black. To download these data, connect to http://stp.wustl.edu/sums/sums.cgi?specfile = 2001-03-02.79O.R.LEWIS_VE_ON_ATLAS.spec

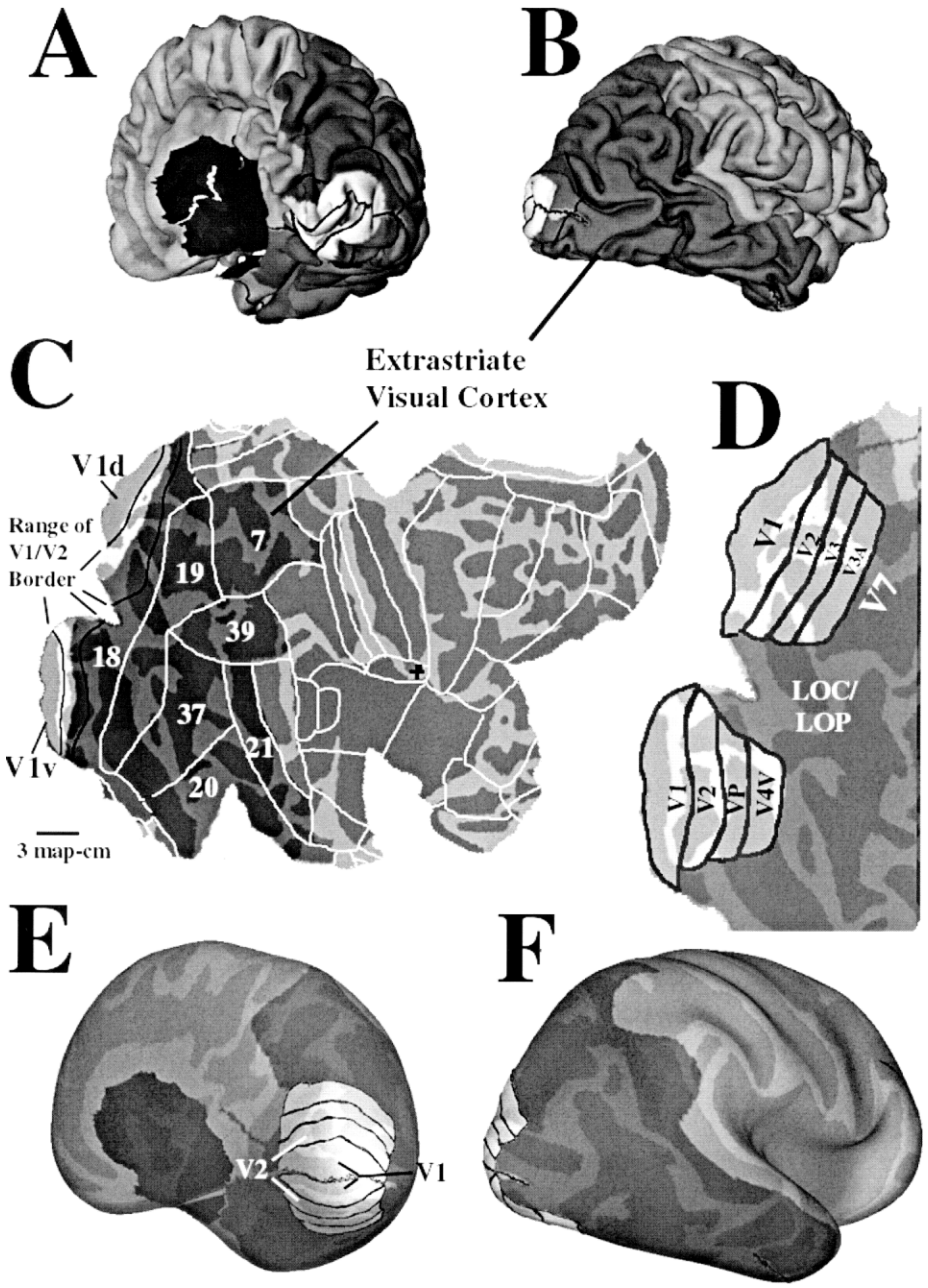

Fig. 5. Human visual cortex and visuotopic areas on the Visible Man surface-based atlas. (A, B) Postero-medial and postero-lateral views of the Visible Man right hemisphere. (C) Flat map of the Visible Man right hemisphere. In panels (A)–(C), dark shading indicates the estimated extent of human visual cortex, light shading indicates the typical extent of area V1, and intermediate shading indicates the cortical geography in non-visual regions. Black lines indicate the approximate upper and lower bounds for the extent of V1 in different individuals (Rademacher et al. 1993). White lines indicate the boundaries of Brodmann's architectonic areas as charted on the Visible Man map (Drury et al., 1999a). (D) Flat map of occipital cortex on the Visible Man atlas, showing the extent of visuotopic areas V1, V2, V3, VP, V3A, and V4v as charted by Van Essen and Drury (1997) and the approximate locations of areas V7 and the LOC/LOP subdivisions of the lateral occipital area as charted by Tootell and Hadjikhani (in press). (E, F) Postero-medial and postero-lateral inflated views of the Visible Man, showing the locations of visuotopic areas. To download these data, connect to http://stp.wustl.edu/sums/sums.cgi?specfile = 2001-02-11.VH.R.ATLAS.BASIC.spec

Van Essen et al., 1984; Van Essen & Drury, 1997). An important but unresolved issue is whether the expanded extent of extrastriate cortex in humans reflects a larger size of individual areas (compared to V1 as a baseline), a greater number of cortical areas, or a combination of both.

Surface-based warping offers an attractive approach for making interspecies comparisons, as it can generate topologically correct mappings from one surface to the other despite the differences in convolutions and in the relative sizes and locations of visual areas. In a previous study, comparisons were made by deforming a flat map

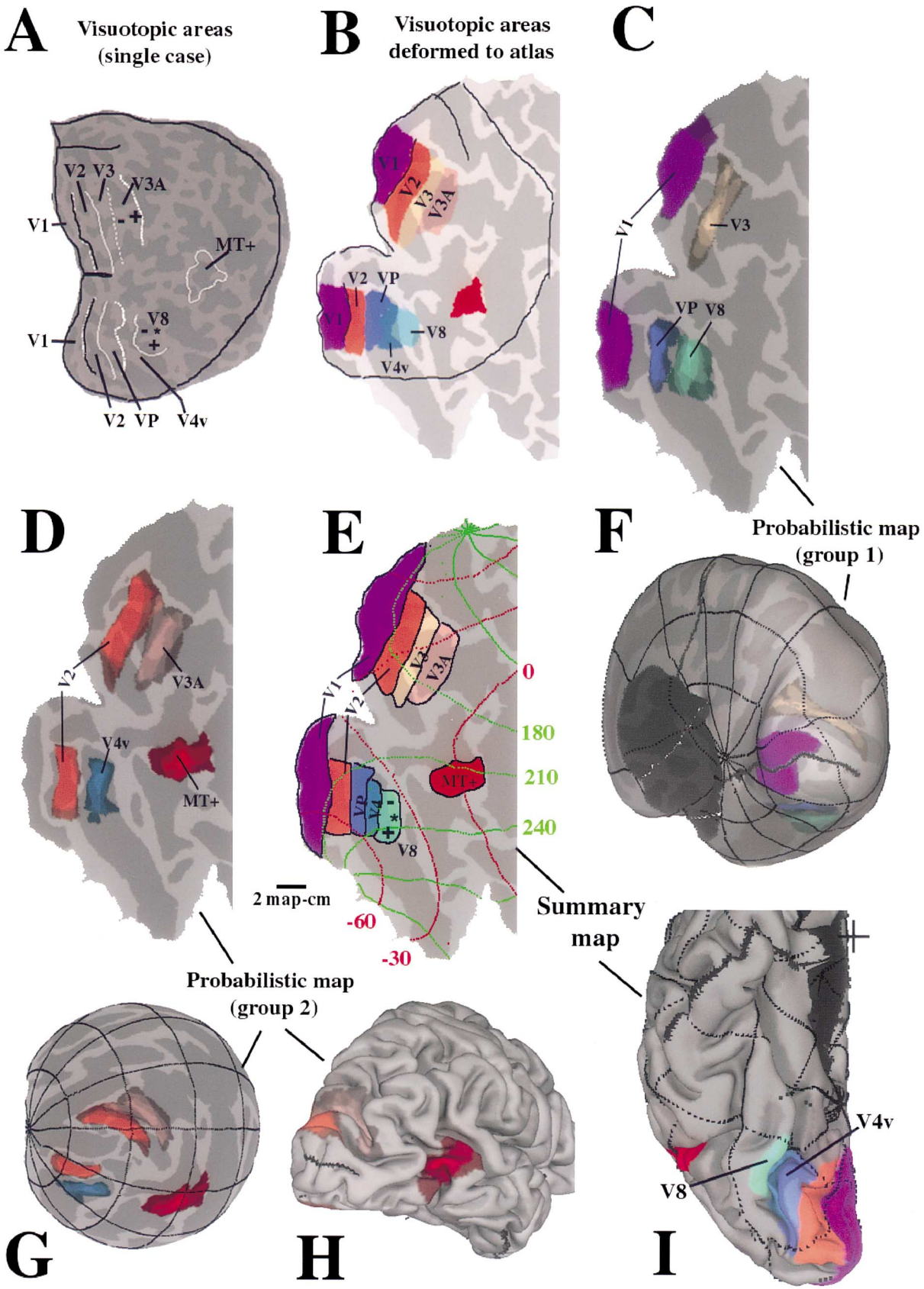
A
Visuotopic areas
(single case)
V2 V3
V3A
V1
MT+
V8
V1
V2 VP V4v
B
Visuotopic areas
deformed to atlas
V1
V2
V3
V3A
V2 VP
V1
V8
V4v
C
V1
V3
VP V8
Probabilistic map
(group 1)
D
V2
V3A
V4v
MT+
E
V1
V2
V3
V3A
0
180
210
240
MT+
VP
V4
V8
2 map-cm
-60
-30
F
Summary
map
V4v
V8
Probabilistic map
(group 2)
G
H
I

Fig. 6.

of a macaque hemisphere to match the shape of the human flat map (Van Essen et al., 1998). That analysis, while informative, was hindered by the necessity of including the artificial cuts used in making the flat maps among the landmarks used to constrain the deformation on the plane. Here, we circumvented this problem using a landmark-based deformation method that operates on spherical maps (Bakircioglu et al., 1999). The distribution of landmark points is shown on the macaque flat map (Fig. 7A) and sphere (Fig. 7B), along with a set of Cartesian grid lines (green and blue) that were carried passively with the deformation. The primary landmarks are indicated by colored squares and interconnecting lines. They include the perimeters of visual areas V1, V2, and MT, shown in blue, green, and orange, respectively. The geographic landmarks include the fundus of the central sulcus (yellow, corresponding to the boundary between primary somatosensory and motor areas); the rhinal sulcus (purple); the juncture between parietal and temporal lobes in the Sylvian fissure (light blue); and the boundaries of neocortex along the medial wall (black, red, and green segments). The small black points indicate secondary landmark points used to stabilize the deformation (i.e. reduce shear and local distortions) in the large expanses between primary landmarks (see Section 2). The deformation brought the source landmarks into precise register with the corresponding target landmarks, as shown on the human spherical map (Fig. 7C) and after projection to the human flat map (Fig. 7D). The deformed grid lines (Fig. 7D) reveal the highly non-uniform pattern of deformation needed to bring the source and target landmarks into register.

The deformation involves about a twofold expansion in surface area for V1 and V2, reflecting the known differences in size for these areas. The expansion is much greater for the rest of the visual cortex, particularly in the parietal lobe. For example, grid square 1 in parietal cortex is expanded about 20-fold in surface area on the flat map of Fig. 7C vs. Fig. 7A. In contrast, grid square 2 in inferotemporal cortex is expanded only about ninefold. The non-uniform expansion of parietal versus temporal regions is driven largely by the fact that MT+ is more ventral and posterior (relative to the axis between foveal V1 and the central sulcus) in humans than in the macaque. Another significant difference is that the gap between anatomically mapped area V1 and the natural margin of neocortex (adjoining the corpus callosum) is considerably greater in humans than macaques. This is evident in the atlases (see Fig. 1F, Fig. 4C, D, Fig. 5C–E, and Fig. 6E) and is indicated by the thin blue arrows in Fig. 7A versus the thick blue arrows in Fig. 7C.

The lower panels in Fig. 7 show the arrangement of macaque visual areas (from the Lewis and Van Essen partitioning scheme of Fig. 4) as they appear on the macaque flat map (Fig. 7E), and sphere (Fig. 7F), and after deformation to the human spherical map (Fig. 7G) and flat map (Fig. 7H). In essence, the map of deformed macaque visual cortex suggests how visual areas might be arranged in human cortex, subject to three explicit assumptions: (i) that the landmarks used to constrain the deformation reflect valid homologies; (ii) that the total number of visual areas and the topological relationships between these areas is similar in humans and macaques; and (iii) that the deformation fields in between the landmarks provide a reasonable approximation to the actual pattern of differential expansion in these regions. Of course, any or all of these assumptions may well be incorrect, but their plausibility is most profitably assessed in the context of specific results for each deformation (see below).

The deformed parietal visual areas are disproportionately expanded on the human map compared to the macaque map, as expected from the aforementioned non-uniformities in the deformation grid. For instance, deformed areas LIPd, LIPv, and the VIP complex collectively occupy both banks of the human intraparietal sulcus, whereas these areas occupy mainly the lateral bank of the intraparietal sulcus in the macaque. In ventral extrastriate cortex, the deformed occipitotemporal areas (including inferotemporal areas TE1-3) are expanded only modestly, reflecting the postero-ventral displacement of MT+ in humans compared to macaques. In more anterior temporal regions, including the deformed TPO complex, the expansion is comparable to that in the parietal lobe, reflecting the larger separation between MT+ and the Sylvian fissure in humans compared to macaques.

Fig. 6. Probabilistic map of human visuotopic areas, based on the fMRI mapping study of Hadjikhani et al. (1998). (A) Map of visuotopic areas from a single case. White lines indicate the boundaries of identified areas on a flat map of occipital and nearby cortical regions. Black lines indicate the landmark contours used to constrain the deformation to the atlas (the V1/V2 boundary, the fundus of the parieto-occipital sulcus, and corresponding segments along the perimeter of each map). (B) Visuotopic areas from the case in (A), after deformation to the Visible Man atlas. (C) Probabilistic map of four visuotopic areas based on four individuals from the Hadjikhani et al. study after deformation to the atlas and displayed on a flat map of occipital cortex. (D) Probabilistic map of the intervening four visual areas displayed on the flat map. (E) Summary map of the most likely boundaries of visual areas, based on the probabilistic maps in panels (C) and (D). (F) Probabilistic map of visual areas (group 1) displayed on a postero-medial view of the inflated hemisphere. (G) Probabilistic map of visual areas (group 2) displayed on the spherical map. (H) Probabilistic map of visual areas displayed on a postero-lateral view of the fiducial surface. (I) Summary map of visuotopic areas displayed on a ventral view of the fiducial surface. To download these data, connect to http://stp.wustl.edu/sums/sums.cgi?specfile = 2001-02-02.VH.R.ATLAS_PROBABILISTIC.spec

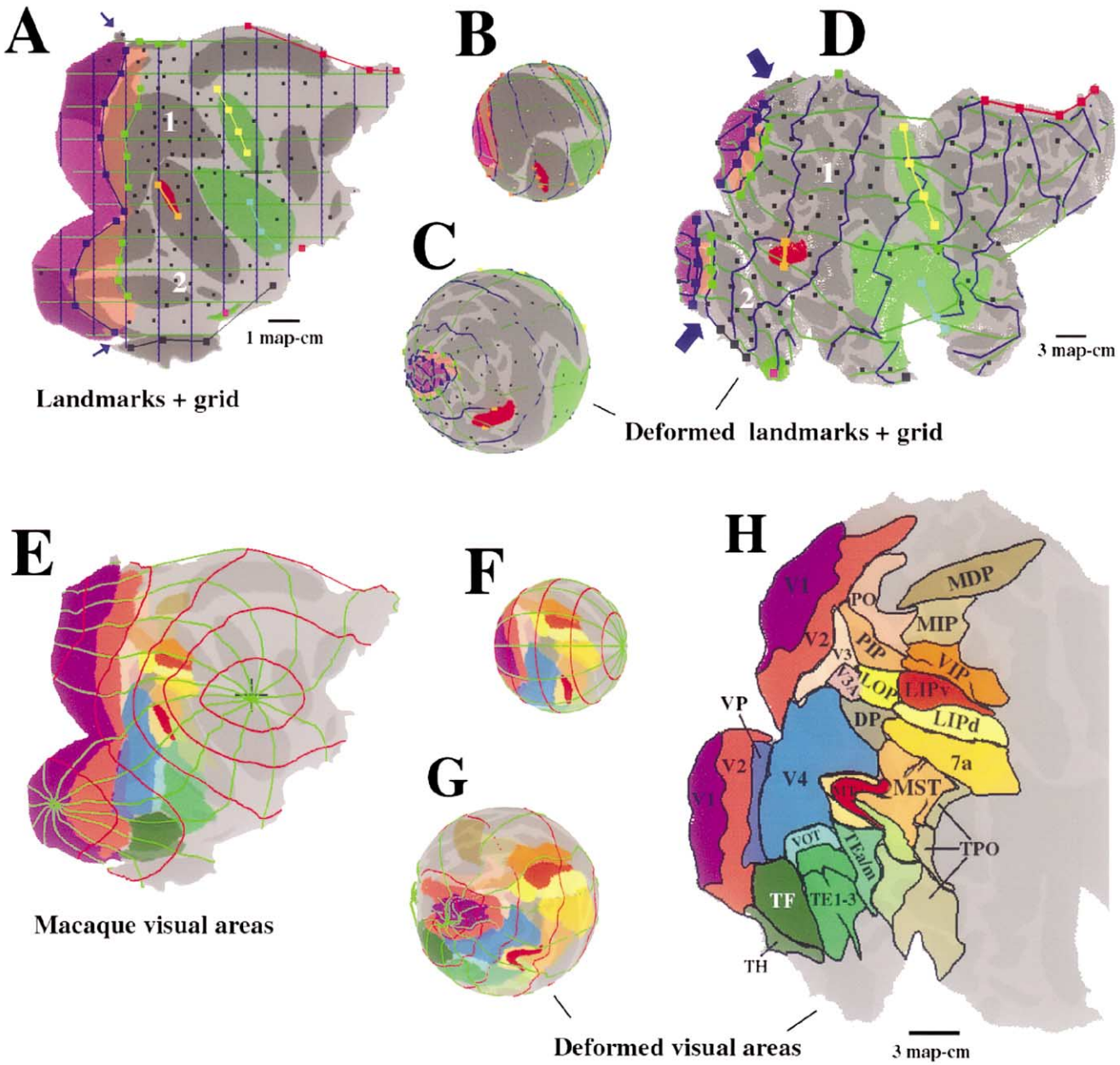

Fig. 7. Interspecies comparisons using surface-based warping from the macaque to the human map. (A) Flat map of the macaque atlas, showing landmarks used to constrain the deformation. These include areas V1, V2, MT+, the central, Sylvian, and rhinal sulci, plus landmarks on the margins of cortex along the medial wall. Grid lines were carried passively with the deformation. (B) Landmarks and grid lines projected to the macaque spherical map. (C) Landmarks and grid lines deformed to the human spherical map. Neither of the spherical maps is at the same scale as the flat maps. (D) Deformed landmarks and grid lines projected to the human flat map. (E) Visual areas on the macaque flat map, based on the Lewis and Van Essen partitioning scheme in Fig. 4, plus iso-latitude and iso-longitude lines. (F) Visual areas on the macaque spherical map, plus iso-latitude and iso-longitude lines. (G) Deformed macaque visual areas on the human spherical map, along with deformed iso-latitude and iso-longitude lines. (H) Deformed macaque visual areas on the human flat map. To download these data, connect to http://stp.wustl.edu/sums/sums.cgi?specfile = 2001-03-06-VH.R.ATLAS_DeformedMa

Fig. 8 illustrates several types of comparisons that can be made between the pattern of deformed macaque visual areas and various types of experimental data available for human occipital, temporal, and parietal cortex. In Fig. 8A, the boundaries of human visuotopic areas (taken from Fig. 6) are overlaid on the pattern of deformed macaque areas. While there are many similarities, there are also many differences between deformed macaque areas and their candidate homologues in humans. Differences that warrant discussion include those relating to areas V2, V3A, MT+/MST, V4, and V8.

Deformed macaque V2 extends substantially farther than human V2 in both directions along its long axis — towards the foveal representation (center of map)

and towards the peripheral representation (top and bottom of map). The discrepancy near the foveal representation probably reflects an incomplete mapping of central vision in the human fMRI data. In contrast, incomplete mapping is unlikely to be a complete explanation for the discrepancy in peripheral V2, which occurs in a region that is disproportionately expanded in humans relative to the macaque (thin versus thick blue arrows in Fig. 7A vs. Fig. 7C). Instead, cortex anterior to V1 may include one or more cortical areas that are relatively large in humans and are absent or very small in macaques. Deformations that take such hypothesized areas into account could result in a deformed macaque V2 in much closer register with the fMRI-based map of human V2.

In dorsal extrastriate cortex, deformed macaque area V3A is much smaller than human V3A. If the homology between V3A in macaques and humans is genuine, this would signify that human V3A is differentially expanded relative to neighboring areas V2 and V3. In

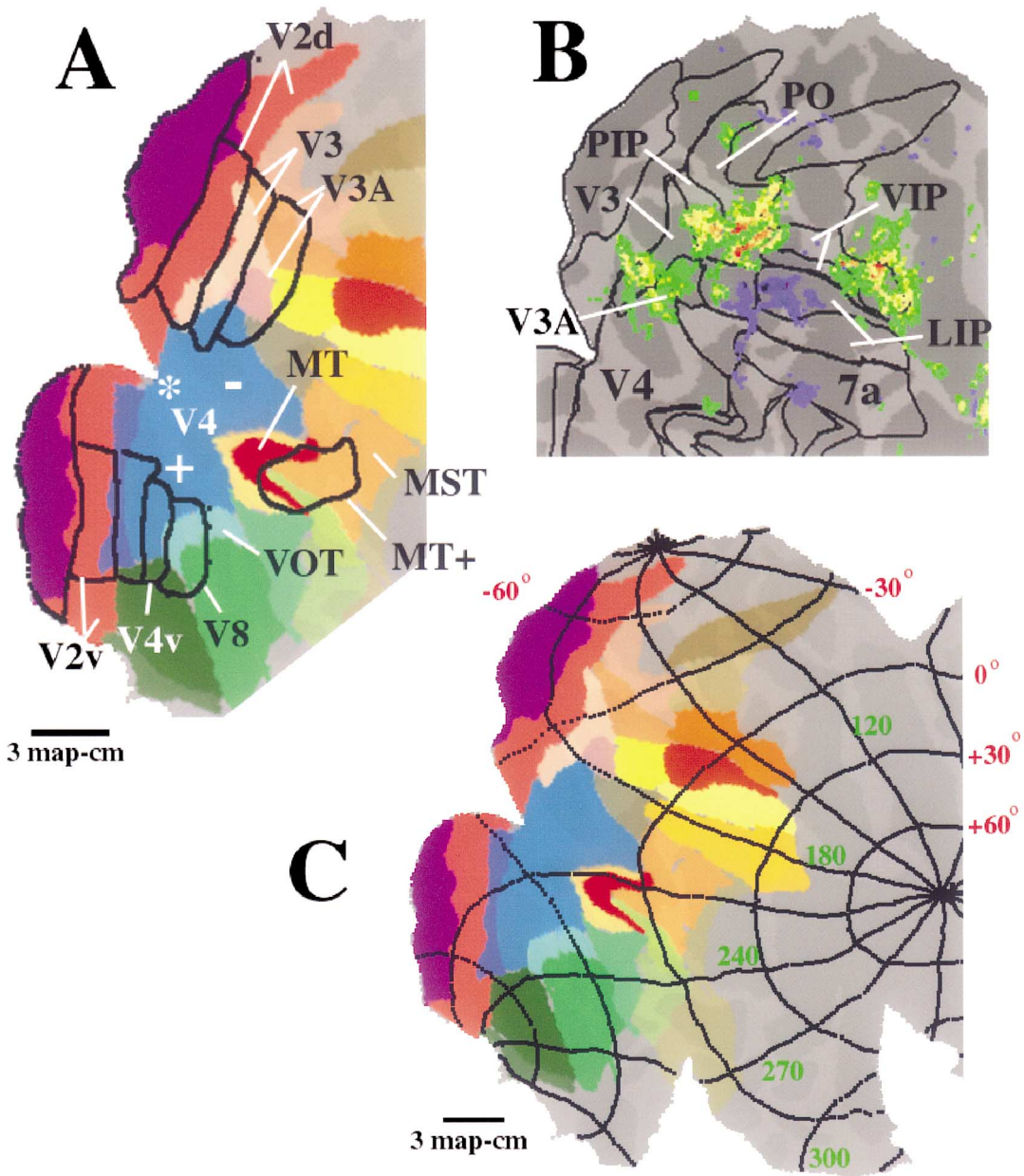

Fig. 8. (A) Boundaries of human visuotopic areas, taken from Fig. 6E, superimposed on a map of deformed macaque visual areas, taken from Fig. 7H. For deformed macaque area V4, the approximate location of the foveal representation (*) and of its lower-field (−) and upper-field (+) representations are indicated. (B) Boundaries of deformed macaque visual areas (black lines) superimposed on the fMRI activation pattern from an attentional task from the study of Corbetta et al. (1998) after deformation to the Visible Man atlas by Drury et al. (1999a). (C) Iso-latitude and iso-longitude lines from the human spherical map projected to the human flat map and superimposed on the map of deformed macaque visual areas.

the vicinity of the MT complex, the deformed macaque MST complex is substantially larger than human MT+, as delineated from motion-specific fMRI activation patterns. A plausible explanation is that the particular fMRI paradigm used to elicit motion-specific responses in humans activates part, but not all, of the human MST complex.

Another important set of comparisons involves the location of deformed macaque V4 in comparison to its candidate homologues in humans. These candidates include V4v, as suggested by Hadjikhani et al. (1998), V8, as suggested by Zeki et al. (1998), and the LOC/LOP complex, as suggested by Tootell and Hadjikhani (in press). In terms of location and approximate size, deformed macaque V4 overlaps most extensively with the human LOC/LOP complex. Deformed ventral V4 also overlaps significantly with human V4v. In addition, the visuotopic organization of human V4v matches that of macaque ventral V4 (Van Essen et al., 1990; Boussaoud, Desimone, & Ungerleider, 1991) in so far as the foveal representation (*) is towards the top and the vertical meridian towards the left on each map. In contrast, the hypothesized correspondence between deformed macaque V4 and human V8 is problematic on several counts. Deformed macaque V4 does not overlap significantly with human V8, and it is much larger in overall extent, even though V8 contains a complete hemifield representation. Consequently, any deformation that brought all of macaque V4 into register with human V8 (while still retaining V1 and V2 as landmarks) would result in very large distortions, particularly in the region between V2 and V4. Moreover, the visuotopic maps of deformed macaque V4 and human V8 have axes that are mirror images of one another. Hence, if these axes are correct, the two maps cannot be brought into register by translation and/or rotation operations alone.

Several of the deformed macaque parietal areas are close to regions in the intraparietal sulcus known from fMRI studies to be associated with both eye movements and shifting attention (Corbetta et al., 1998). Because fMRI activation patterns are often complex and irregular, it is useful to analyze the full activation patterns rather than just the centers of activation hot spots. To that end, Fig. 8B shows the boundaries of deformed macaque parietal and dorsal occipital areas superimposed on an fMRI activation pattern taken from the attentional task of Corbetta et al. (1998) after the data were deformed to the Visible Man atlas (Drury et al., 1999a). There are three main patches of positive activation (shown in green, yellow, and red), including one in the anterior intraparietal sulcus that overlaps extensively with deformed macaque VIP, another that overlaps mainly with deformed areas PIP and PO, and a third that overlaps mainly with deformed V3 and V3A. None of the positive activation foci overlap significantly with deformed LIPv or LIPd, despite neurophysiological evidence that neuronal responses in macaque LIP are modulated by attention as well as eye movements (Andersen, 1989; Colby & Goldberg, 1999). This could signify that the behavioral task was not suited for activating human LIP neurons. Equally plausibly, it may signify that the deformation constraints led to an inaccurate positioning for the deformed LIP complex, and that alternative constraints may be needed to bring homologous areas into alignment in parietal cortex.

Surface-based coordinates can be used as a more general tool for facilitating interspecies comparisons. Fig. 8C shows lines of constant latitude and longitude from the human map superimposed on the map of deformed macaque visual areas. Any experimental data that have been reported by their spherical coordinates on the Visible Man atlas can be directly compared to the map of deformed macaque areas using the coordinates shown in this panel.

4. Discussion

The utility of surface reconstructions in enhancing our understanding of visual cortex has been amply demonstrated over the past 5 years by numerous studies in which results were displayed and analyzed on individual experimental hemispheres in humans (e.g. Sereno et al., 1995; DeYoe et al., 1996; Tootell, Dale, Sereno, & Malach, 1996; Tootell et al., 1997; Tootell, Hadjikhani, Mendola, Marrett, & Dale, 1998) and macaques (Hadjikhani et al., 1998; Lewis & Van Essen, 2000a,b). The trend towards surface-based analyses will surely accelerate now that automated methods for surface reconstruction, manipulation, and visualization have recently become generally available.

The present study has emphasized the role of surface-based atlases in complementing and extending the analyses that can be made on individual surface reconstructions. In general, atlases provide a natural framework for identifying commonalities between individuals, for assessing the magnitude of individual differences, and for comparing disparate types of information derived from many different sources. Surface-based atlases, as distinct from conventional volume-based atlases, are essential for capitalizing on the inherent visualization advantages associated with surface reconstructions and the inherent registration advantages associated with surface-based warping (see Van Essen et al., 1998; Drury et al., 1999a,b; Fischl et al., 1999b).

One method of surface-based warping, pioneered by Fischl et al. (1999b) constrains the warping from individual spherical maps onto an atlas sphere using a measure of cortical shape (local surface convexity) that is derived objectively and automatically across the en-

tire cortical surface. The landmarked-based approach used in the present study differs in that it allows any desired combination of geographic and functional landmarks to constrain the deformation, though at the price of requiring explicit designation of landmarks for each hemisphere undergoing deformation. In evaluating these two approaches, along with any alternative methods or hybrid approaches that are developed in the future, several general considerations should be borne in mind. Within the general framework of surface-based warping, there are an infinite number of possible ways to deform one map to another, and the preferred choice depends upon the questions being addressed as well as the experimental data that are available. For example, the question of whether specific functional landmarks, such as the boundaries of particular visual areas (V1, etc.) should be included among the deformation constraints depends upon (i) the availability of information about these boundaries for all of the hemispheres to be deformed and (ii) the desirability of using these constraints to factor out one source of variability versus the desirability of analyzing that particular source of variability in its own right. In general, the nature of individual variability in cortical structure and function implies that there is no "gold standard" basis for determining what constitutes precisely corresponding locations in different hemispheres. Consequently, surface-based atlases in the future are likely to contain a multiplicity of probabilistic atlases that reflect different criteria used for deformation as well as different data sets that are deformed.

The atlases illustrated here for both macaque and human represent early stages of what will be rapidly evolving and expanding families of probabilistically based atlases. The macaque atlas is the more advanced, as it provides detailed maps for a wider expanse of visual cortex, and it contains multiple summary maps representing different partitioning schemes and based on a variety of types of data. Besides the two schemes illustrated here (the predominantly architectonic scheme of Lewis and Van Essen and the composite scheme of Felleman and Van Essen), the partitioning schemes of Brodmann (1909), von Bonin and Bailey (1947) and Desimone & Ungerleider (1986) have all been deformed to this atlas as well (Drury, Van Essen, Joshi, & Miller, 1996b). Thus, it represents a centralized repository for addressing a variety of unresolved issues about the identification of different visual areas. Emerging results from neurophysiological, anatomical, and neuroimaging studies can be incorporated into this atlas, using surface-based warping whenever feasible; competing partitioning schemes can then be evaluated with regard to their consistency with the newly incorporated findings.

The atlas of human visual cortex is currently more rudimentary, as we have focussed initially on obtaining accurate maps for the modest number of identified visuotopic areas. This situation will change drastically as existing and newly acquired information about various functional specializations derived from fMRI, MEG, and other neuroimaging methods is incorporated into the atlas. However, the complexity of these neuroimaging data will give rise to a number of challenges in dealing with data from diverse types of experiments as well as many different individuals. Of particular importance is the recognition that the occurrence of a patch of activation associated with one or another behavioral task does not necessarily imply the existence of a specific cortical area devoted to that task. While the interpretative challenges remain daunting, the options for addressing them systematically and objectively will be aided by having maps of activation patterns from a variety of behavioral tasks brought into register on the atlas, so that comparisons can be based on full patterns of activation rather than just the coordinates of the activation centers.

With regard to interspecies comparisons, the surface-based approach illustrated here is not intended to prove or disprove any particular homologies on its own. Rather, it aims to provide a useful spatial framework to facilitate objective comparisons and to allow exploration of the implications of any one set of proposed homologies on candidate homologies in nearby regions of cortex. For example, the proposed homology between human and macaque MT+ has strong implications regarding the organization of visual areas in nearby parietal and temporal extrastriate cortex, owing to the ventral displacement of human MT+ relative to its location in the macaque. Any number of alternative hypotheses involving different sets of candidate homologies and correspondences can be explored within this framework in order to see which hypotheses account best for the overall match of experimental data for the two species.

The increasing use of surface-based analyses and surface-based atlases has major implications for how data are stored, accessed, and visualized by the neuroscience community.

1. *Data storage and access*. It is increasingly important to have a means for systematically storing surface reconstructions and surface-related data in ways that take into account the intrinsic structure of the data. One effort in this direction is the Surface Management System (SuMS), a database for cortical surfaces and surface-related data, including the atlases described in the present report (Dickson, Drury, & Van Essen, in press). SuMS provides a centralized repository designed for easy entry and web-based retrieval of closely linked data sets, such as the multiple configurations (flat maps, inflated maps, and spherical maps) used to visualize any given hemisphere plus specific experimental data

(e.g. fMRI activation patterns) associated with that surface. The hyperlinks in the figure legends of the present study illustrate the utility of this approach.

2. *Interactive data visualization*. Static images such as those in conventional scientific publications can display only a small fraction of the information contained in a surface-based atlas. Interactive software packages for surface visualization have major advantages for accessing these increasingly complex data sets. For example, the Caret software used extensively in the present study is freely available, runs on multiple platforms (SGI, Solaris, Linux), and includes a wide variety of interactive visualization options for examining individual data sets and making comparisons between different types of experimental data. While much can be accomplished with this and other currently available surface visualization packages, there are many additional capabilities that await future developments in brain-mapping software. These hold great promise for dramatically increasing our understanding of the structure and function of primate visual cortex.

Acknowledgements

This work was supported by NEI grant EY02091 to D.V.E., a Human Brain Project/Neuroinformatics research grant funded jointly by the National Institute of Mental Health, National Science Foundation, National Cancer Institute, National Library of Medicine and the National Aeronautics and Space Administration (R01 MH60974-06) to D.V.E., and MIM and NEI EY09258 to R.B.H.T. We thank James Dickson and John Harwell for brain-mapping software development and Susan Danker for assistance in manuscript preparation.

References

Amunts, K., Malikovic, A., Mohlberg, H., Schormann, T., & Zilles, K. (2000). Brodmann's areas 17 and 18 brought into stereotaxic space — Where and how variable? *NeuroImage*, *11*, 66–84.

Andersen, R. A. (1989). Visual and eye movement functions of the posterior parietal cortex. *Annu. Rev. Neurosci.*, *12*, 377–403.

Bakircioglu, M., Joshi, S., & Miller, M. I. (1999). Landmark matching on the sphere via large deformation diffeomorphisms. In *Proceedings of SPIE Medical Imaging. Image Processing*, vol. 3661 (pp. 710–715).

Boussaoud, D., Desimone, R., & Ungerleider, L. G. (1991). Visual topography of area TEO in the macaque. *J. Comp. Neurol.*, *306*, 554–575.

Brodmann, K. (1909). *Vergleichende Lokalisationslehre der Grosshirnrinde in ihren Prinzipien dargestellt auf Grund des Zellenbaues*. Leipzig: J.A. Barth.

Carman, G. J., Drury, H. A., & Van Essen, D. C. (1995). Computational methods for reconstructing and unfolding the cerebral cortex. *Cerebral Cortex*, *5*, 506–517.

Colby, C. L., & Goldberg, M. E. (1999). Space and attention in parietal cortex. *Annu. Rev. Neurosci.*, *22*, 319–349.

Corbetta, M., Akbudak, E., Conturo, T. E., Snyder, A. Z., Ollinger, J. M., Drury, H. A., Linenweber, M. R., Raichle, M. E., Van Essen, D. C., Petersen, S. E., & Shulman, G. L. (1998). A common network of functional areas for attention and eye movements. *Neuron*, *21*, 761–773.

Dale, A. M., Fischl, B., & Sereno, M. I. (1999). Cortical surface-based analysis. I. Segmentation and surface reconstruction. *NeuroImage*, *9*, 179–194.

Desimone, R., & Ungerleider, L. B. (1986). Multiple visual areas in the caudal superior temporal sulcus of the macaque. *J. Comp. Neurol.*, *248*, 164–189.

DeYoe E. A. (in press). The human occipal lobe. In: V. S. Ramachandran (Ed.), The encyclopedia of the human brain. New York: Academic Press.

DeYoe, E. A., Hockfield, S., Garren, H., & Van Essen, D. C. (1990). Antibody labeling of functional subdivisions in visual cortex: Cat-301 immunoreactivity in striate and extrastriate cortex of the macaque monkey. *Vis. Neurosci.*, *5*, 67–81.

DeYoe, E. A., Carman, G., Bandetinni, P., Glickman, S., Wieser, J., Cox, R., Miller, D., & Neitz, J. (1996). Mapping striate and extrastriate visual areas in human cerebral cortex. *Proc. Natl. Acad. Sci. USA*, *93*, 2382–2386.

Dickson, J., Drury, H., & Van Essen, D. C. (in press) Surface management system (SuMS): A surface-based database to aid cortical surface reconstruction, visualization and analysis. Phil. Trans. R. Soc. Ser. B.

Drury, H. A., Van Essen, D. C., Anderson, C. H., Lee, C. W., Coogan, T. A., & Lewis, J. W. (1996a). Computerized mappings of the cerebral cortex. A multiresolution flattening method and a surface-based coordinate system. *J. Cogn. Neurosci.*, *8*, 1–28.

Drury, H. A., Van Essen, D. C., Joshi, S. C., & Miller, M. I. (1996b). Analysis and comparison of areal partitioning schemes using two-dimensional fluid deformations. *NeuroImage*, *3*, S130.

Drury, H. A., Van Essen, D. C., Corbetta, M., & Snyder, A. Z. (1999a). Surface-based analyses of the human cerebral cortex. In A. Toga, et al., *Brain Warping* (pp. 337–363). New York: Academic Press.

Drury, H. A., Van Essen, D. C., & Lewis, J. W. (1999b). Towards probabilistic surface-based atlases of primate cerebral cortex. *Soc. Neurosci. Abstr.*, *25*, 1929.

Felleman, D. J., & Van Essen, D. C. (1991). Distributed hierarchical processing in primate cerebral cortex. *Cerebral Cortex*, *1*, 1–47.

Fischl, B., Sereno, M. I., & Dale, A. M. (1999a). Cortical surface-based analysis. II: Inflation, flattening, and a surface-based coordinate system. *NeuroImage*, *9*, 195–207.

Fischl, B., Sereno, M. I., Tootell, R. B., & Dale, A. M. (1999b). High-resolution intersubject averaging and a coordinate system for the cortical surface. *Hum Brain Mapp.*, *8*(4), 272–284.

Goebel, R. (2000). A fast automated method for flattening cortical surfaces. *NeuroImage*, *11*, S680.

Hadjikhani, N., Liu, A. K., Dale, A. M., Cavanagh, P., & Tootell, R. B. H. (1998). Retinotopy and color sensitivity in human visual cortical area V8. *Nat. Neurosci.*, *1*, 235–241.

Horton, J. C., & Hubel, D. H. (1991). Regular patchy distribution of cytochrome oxidase staining in primary visual cortex of macaque monkey. *Nature*, *292*, 762–764.

Joshi, S. C. (1997) Large deformation landmark based differeomorphic for image matching. Ph.D. thesis, Sever Institute, Washington University, September.

Kiebel, S., Goebel, R., & Friston, K. (2000). Anatomically informed basis functions. *NeuroImage*, *11*, 656–667.

Lancaster, J. L., Glass, T. G., Lankipalli, B. R., Downs, H., Mayberg, H., & Fox, P. T. (1995). A modality-independent approach to spatial normalization of tomographic images of the human brain. *Hum. Brain Mapp.*, *3*, 209–223.

Lewis, J. W. & Van Essen, D. C. (2000a) Architectonic parcellation of parieto-occipital cortex and interconnected cortical regions in the Macaque monkey, J. Comp. Neurol. (in press).

Lewis, J. W. & Van Essen, D. C. (2000b) Cortico-cortical connections of visual, sensorimotor, and multimodal processing areas in the parietal lobe of the Macaque monkey. J. Comp. Neurol. (in press).

Ono, M., Kubick, S., & Abernathey, C. D. (1990). *Atlas of the cerebral sulci*. New York: Thieme Medical.

Rademacher, J., Caviness Jr, V. S., Steinmetz, H., & Galaburda, A. M. (1993). Topographical variation of the human primary cortices: Implications for neuroimaging, brain mapping, and neurobiology. *Cerebral Cortex*, *3*, 313–329.

Rockland, K. S., Kaas, J. H., & Peters, A. (1997). *Extrastriate cortex in primates*. In: *Cerebral cortex*, vol. 12. New York: Plenum Press.

Sereno, M. I., Dale, A. M., Liu, A., & Tootell, R. B. H. (1996). A surface-based coordinate system for a canonical cortex. *NeuroImage*, *3*, S252.

Sereno, M. I., Dale, A. M., Reppas, J. B., Kwong, K. K., Belliveau, J. W., Bardy, T. J., Rosen, B. R., & Tootell, R. B. H. (1995). Borders of multiple visual areas in humans revealed by functional magnetic resonance imaging. *Science*, *268*, 889–893.

Spitzer, V., Ackerman, M. J., Scherzinger, A. L., & Whitlock, D. J. (1996). The Visible Male: a technical report. *J. Am. Med. Inform. Assoc.*, *3*, 118–130.

Steinmetz, H., Furst, G., & Freund, H. J. (1990). Variation of perisylvian and calcarine anatomic landmarks within stereotaxic proportional coordinates. *Am. J. Neuroradiol*, *11*, 1123–1130.

Talairach, J., & Tournoux, P. (1988). *Coplanar stereotaxic atlas of the human brain*. New York: Thieme Medical.

Tootell, R. B. H. & Hadjikhani, N. (in press) Where is ''dorsal V4'' in human visual cortex? Retinotopic, topographic and functional evidence. Cerebral Cortex.

Tootell, R. B. H., & Hamilton, S. L. (1989). Functional anatomy of the second cortical visual area (V2) in the macaque. *J. Neurosci.*, *9*, 2620–2644.

Tootell, R. B. H., Dale, A. M., Sereno, M. I., & Malach, R. (1996). New images from human visual cortex. *Trends Neurosci*, *19*, 481–489.

Tootell, R. B. H., Mendola, J. D., Hadjikhani, N. K., Ledden, P. J., Liu, A. K., Reppas, J. B., Sereno, M. I., & Dale, A. M. (1997). Functional analysis of V3A and related areas in human visual cortex. *J. Neurosci.*, *17*, 7060–7078.

Tootell, R. B. H., Hadjikhani, N. K., Mendola, J. D., Marrett, S., & Dale, A. M. (1998). From retinotopy to recognition: fMRI in human visual cortex. *Trends Cognit. Sci.*, *2*, 174–183.

Van Essen, D. C., & Drury, H. A. (1997). Structural and functional analyses of human cerebral cortex using a surface-based atlas. *J. Neurosci.*, *17*, 7079–7102.

Van Essen, D. C., Newsome, W. T., & Maunsell, J. H. R. (1984). The visual field representation in striate cortex of the macaque monkey: asymmetries, anisotropies and individual variability. *Vision Res.*, *24*, 429–448.

Van Essen, D. C., Felleman, D. F., DeYoe, E. A., Olavarria, J. F., & Knierim, J. J. (1990). Modular and hierarchical organization of extrastriate visual cortex in the macaque monkey. *Cold Spring Harbor Symp. Quant. Biol.*, *55*, 679–696.

Van Essen, D. C., Drury, H. A., Joshi, S., & Miller, M. I. (1998). Functional and structural mapping of human cerebral cortex: Solutions are in the surfaces. *Proc Natl. Acad. Sci. USA*, *95*, 788–795.

Van Essen, D. C., Drury, H. A., & Anderson, C. H. (1999). An automated method for accurately reconstructing the cortical surface. *NeuroImage*, *9*, 173.

von Bonin, G., & Bailey, P. (1947). *The neocortex of Macaca mulatta*. Urbana, IL: University of Illinois.

Wandell, B. A., Chial, S., & Backus, B. T. (2000). Visualization and measurement of the cortical surface. *J. Cogn. Neurosci.*, *12*, 739–752.

Zeki, S., McKeefry, D. J., Bartels, A., & Frackowiak, R. S. J. (1998). Has a new color been discovered? *Nature Neuroscience*, *1*, 335–336.